Relationship between Viscoelastic Relaxation Function and Segmental Displacement Function for Entangled Linear Chain in Early Stage of the Tube Dilation Process

Hiroshi Watanabe* and Alok K. R. Paul

Institute for Chemical Research, Kyoto University, Uji, Kyoto 611-0011 Japan

Received July 25, 2002

ABSTRACT: For highly entangled linear chains, the mean-square displacement of the primitive chain segments $[d(n,t)]^2$ (n = segment index) not including a contribution from a nondiffusive part of the contour length fluctuation (CLF) was analyzed on the basis of the tube concept. The analysis was made by just considering the Gaussian nature of the chains (without detailed assumptions about the chain motion). A simple analytic relationship between this $[d(n,t)]^2$ and the normalized viscoelastic relaxation function $\mu(t)$ was derived in a range of $\mu(t) > 0.5$ and at t longer than the Rouse time τ_{Rouse} for CLF. This relationship was significantly affected by the dynamic tube dilation (DTD) mechanism. For example, the end segment exhibited $d^2 = \langle R^2 \rangle (1 - \mu)$ in the absence of DTD and $d^2 \cong \langle R^2 \rangle (1 - \mu^{1/2})$ in the presence of DTD, with $\langle R^2 \rangle$ being the mean-square end-to-end distance of the chain. This difference should enable a test of the DTD picture at short t (but still longer than τ_{Rouse}) through comparison of the viscoelastic and segmental displacement data.

1. Introduction

The dynamic tube dilation (DTD)[1−3] is one of the most important mechanisms incorporated in current tube models for entangled chains. The DTD is equivalent to the mutual equilibration of successive entanglement segments in a given chain due to the constraint-release-(CR-) induced motion, i.e., the motion activated by the movement of the surrounding chains.

The tube models combining the DTD and other mechanisms (such as the contour length fluctuation; CLF) considerably well describe the linear *viscoelastic* data of entangled chains.[4−6] However, it should be emphasized that the viscoelastic property reflects just a particular aspect of the chain dynamics, the decay of the *isochronal* orientational anisotropy.[3,7] In other words, the agreement between the viscoelastic data and the model prediction does not necessarily guarantee that the chain actually moves in a way assumed in the models.

From this point of view, it is important to compare dynamic properties that differently average the same stochastic chain motion. Indeed, we recently compared the viscoelastic and dielectric properties of *cis*-polyisoprene (PI) chains to examine the validity of the DTD picture.[8−12] The PI chains have the type-A dipoles parallel along the chain backbone, and the global chain motion induces the dielectric relaxation. For the PI chains without dipole inversion, this relaxation detects the orientational correlation of the entire chain at two *separate* times (e.g., 0 and t). Thus, the stochastic chain motion is differently averaged in the dielectric and viscoelastic properties.

In the DTD picture, the relaxed portion of the chain is regarded to behave as a simple solvent and the tube diameter is fully dilated to $a'(t) = a\{\varphi'(t)\}^{-\alpha/2}$ at a time t. Here, a is the diameter of the nondilated tube, $\varphi'(t)$ is the survival fraction of the dilated tube at t, and α (=1−1.3) is a dilation exponent. To test this DTD picture, we derived a relationship between the *normalized* dielectric and viscoelastic relaxation functions,[8,9,11,12] $\Phi(t)$ and $\mu(t)$ ($=G(t)/G_N$),

$$\mu(t) \cong [\Phi(t)]^{1+\alpha} \quad (+ \text{ tube-edge correction term}^{11,12}) \tag{1}$$

This DTD relationship was derived from a general consideration about the tube survival fraction and the Gaussian feature of the chain, without assuming any details of the chain motion. Thus, this relationship holds whenever the tube diameter dilates to $a' = a\{\varphi'(t)\}^{-\alpha/2}$ and the chain moves in this dilated tube.

The comparison of the viscoelastic and dielectric data revealed the validity of eq 1 for monodisperse linear PI[8,11,12] at long t and the failure for monodisperse star PI.[9−12] Thus, the monodisperse linear chain quite possibly moves in the dilated tube of the diameter a' in the *terminal relaxation regime*, but this is not the case for the star chains. This failure of the DTD picture for the star chains in the terminal regime is attributable to an *insufficient* tube dilation (to a diameter $< a\{\varphi'(t)\}^{-\alpha/2}$) that reflects a broad distribution of the motional modes of the star arm.[9−12]

In relation to the above results, we note that the DTD picture might have failed even for the monodisperse linear chain at short t where the chain has the equilibrated contour length but exhibits rather short-ranged motion: At short t, only insufficient tube dilation might have occurred also for the linear chain.

We can examine, *in principle*, this failure at short t by testing the validity of eq 1 for the viscoelastic $\mu(t)$ and dielectric $\Phi(t)$. However, we may have a *practical difficulty* in this test. The $\mu(t)$ and $\Phi(t)$ to be utilized in the test represent the relaxation *due only to* the global chain motion, while the viscoelastic and dielectric data measured at *short t* include contributions from the fast, local motion of monomeric segments within the entanglement segment. Thus, for the test of the DTD picture at short t, we have to subtract these contributions from the measured data to evaluate $\mu(t)$ and $\Phi(t)$. (For long chains at long t, the local motion negligibly contributes to the data and the DTD picture can be

* To whom correspondence should be addressed.

10.1021/ma021200t CCC: $25.00
Published on Web 03/11/2003

tested without this subtraction. However, the subtraction is essential in the test at short t.)

For the viscoelastic data, the contribution of the local motion can be subtracted with the aid of the modified stress−optical rule (MSOR),[13−15] and the $\mu(t)$ due only to the global motion can be evaluated with satisfactory accuracy. However, it is not easy to make a similarly accurate subtraction for the dielectric data: For most of type-A chains (including PI) at short t, the local motion of the monomeric segments is dielectrically active because of their type-B dipoles perpendicular to the chain backbone. A rule being analogous to the MOSR and enabling an accurate subtraction of this type-B contribution is not available. Consequently, the $\Phi(t)$ obtained after this subtraction always includes a nonnegligible uncertainty at short t.[3] The *normalized* relaxation functions $\mu(t)$ and $\Phi(t)$ are close to unity at short t in any case, and this uncertainty may disturb us to experimentally distinguish the two relationships, $\mu(t) = [\Phi(t)]^{1+\alpha}$ (in the presence of DTD, eq 1) and $\mu(t) = \Phi(t)$ (in the absence of DTD).

Thus, for the test of the DTD picture without this practical difficulty, we should choose viscoelastic and *nondielectric* properties (the latter being accurately measurable at short t) and formulate their DTD and non-DTD relationships that are experimentally distinguishable at short t. We looked for various nondielectric properties and found that the mean-square displacement of *primitive chain segments*, $[d(n,t)]^2$ (with n = segment index), is a good candidate to be utilized in the test: From the mean-square displacement measured for the monomeric segments, a difference $[d(n,t)]^2 - [d(n',t)]^2$ ($n \neq n'$) can be straightforwardly evaluated.

Focusing on this feature of $[d(n,t)]^2$, we considered just the Gaussian feature of the chain to formulate the DTD and non-DTD relationships between $\mu(t)$ and $[d(n,t)]^2$ at short t. These relationships, written in simple forms in particular for the primitive chain segments at the chain end, were easily distinguishable at short t and served as a basis of our test of the DTD picture. In this paper, we present these results and discuss a possible experimental mode of this test.

2. Definition of Analyzed/Calculated Quantities

We consider a monodisperse system of highly entangled linear chains at equilibrium. The entanglement constraint is represented by the tube. A primitive chain, defined as a curvilinear axis of the chain along the nondilated tube,[7] is composed of N ($\gg 1$) segments referred to as the *primitive segments*. The mean-square end-to-end distance of the chain is given by $\langle R^2 \rangle = Na^2$, where a is the primitive segment size that coincides with the diameter of the nondilated tube. Throughout this paper, we neglect a difference between N and $N - 1$ (number of the bonds connecting neighboring primitive segments.).

We focus on the mean-square displacement $[\mathscr{D}(n,t)]^2$ of the nth primitive segment in an interval of time between 0 and t. (A relationship between this $\mathscr{D}^2$ and the mean-square displacement measured for the monomeric segments is explained later in relation to the experimental mode of the test of the DTD picture.) The time scale t considered here is longer than the Rouse time τ_{Rouse} for the thermal contour length fluctuation (CLF) along the nondilated tube, but shorter than the terminal viscoelastic relaxation time τ_G to an extent that the Fickian diffusion of the chain (giving $\mathscr{D}^2 \propto t$) is negligible. In this time scale, the real chain can be safely coarse-grained into the primitive chain having a constant contour length aN, and $[\mathscr{D}(n,t)]^2$ can be written as $[\mathscr{D}(n,t)]^2 = [d(n,t)]^2 + d_{\text{CLF}}{}^2$. Here, $d_{\text{CLF}}{}^2$ is the mean-square displacement due only to a nondiffusive part of CLF, i.e., the part without the curvilinear diffusion along the tube.[7] (The displacement due to this curvilinear diffusion is included in $[d(n,t)]^2$.)

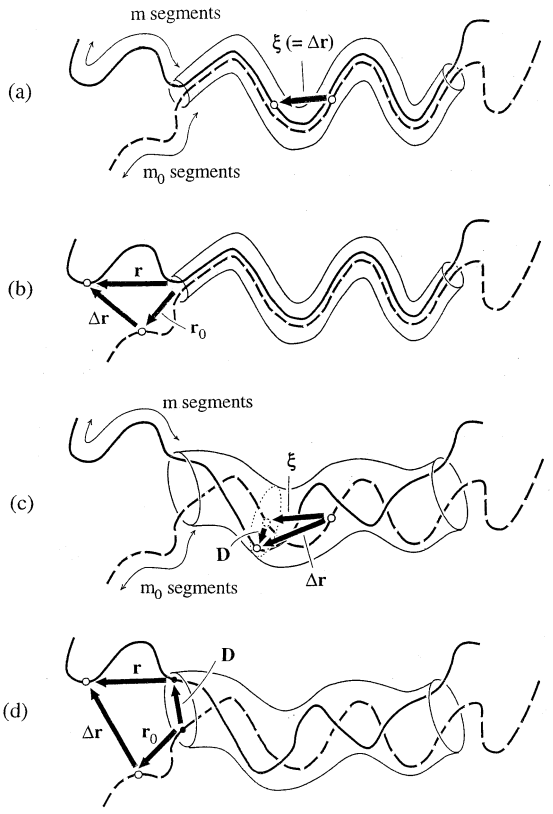

Figure 1. Schematic illustration of the primitive chain moving in the fixed tube (parts a and b) and in the dilated tube (parts c and d). The dashed and solid curves represent the chain at the times 0 and t, respectively. The unfilled circles indicate the nth primitive segment that exhibits a displacement $\Delta\boldsymbol{r}$ in the interval of time between 0 and t. (This $\Delta\boldsymbol{r}$ does not include a contribution from the nondiffusive part of CLF.) For further details, see text.

The $[d(n,t)]^2$ ($= [\mathscr{D}(n,t)]^2 - d_{\text{CLF}}{}^2$) is defined in terms of the displacement vector $\Delta\boldsymbol{r}(n,t)$ of the nth primitive segment in an interval of time between 0 and t ($> \tau_{\text{Rouse}}$)

$$[d(n,t)]^2 = \langle [\Delta\boldsymbol{r}(n,t)]^2 \rangle \tag{2}$$

Here, $\langle \cdots \rangle$ represents an ensemble average taken for the chains in the system. This $\Delta\boldsymbol{r}(n,t)$ is defined to be not contributed from the nondiffusive part of CLF. In this paper, we analyze $\Delta\boldsymbol{r}(n,t)$ to calculate $[d(n,t)]^2$.

In Figure 1, the dashed and solid curves represent the primitive chain at the times 0 and t, respectively. Parts a and b schematically show the changes of the conformation of the chain trapped in a spatially fixed (nondilated) tube, and the parts c and d indicate the conformational changes for the case of DTD. As can be noted from these changes, $\Delta\boldsymbol{r}(n,t)$ reflects the longitudinal motion of the primitive segment along the fixed/dilated tube and the lateral motion in the dilated tube. Considering the Gaussian feature of the chain, we can characterize $\Delta\boldsymbol{r}(n,t)$ in terms of the survival fraction of either the fixed or dilated tube to calculate $[d(n,t)]^2$ and derive a relationship between $[d(n,t)]^2$ and $\mu(t)$.

In this derivation, we make no detailed assumption about the chain motion between the times 0 and t so that the obtained relationship can have the maximum generality. (If we assume a time evolution equation for the primitive segment position, we can explicitly calculate $[d(n,t)]^2$ and $\mu(t)$ as functions of t and obtain a relationship between $[d(n,t)]^2$ and $\mu(t)$ by erasing t. However, in this paper, we do not use this approach.)

In principle, the tube survival fraction has a distribution among the chains in the system. However, in the analysis presented here, the survival fraction is regarded to be the same for all chains. This is the largest approximation in this paper.

Our aim is to formulate the relationship between $[d(n,t)]^2$ and $\mu(t)$ for the two cases of the presence and absence of DTD and discuss an experimental mode for the test of the DTD picture at short t (but still longer than τ_{Rouse}). The formulation for the case of DTD is based on that for the case of the fixed tube. Thus, the relationship between $[d(n,t)]^2$ and $\mu(t)$ for the latter case is first explained below. Then, the result is utilized to derive the relationship for the former case.

3. Relationship between d^2 and μ for the Chain in a Fixed Tube

3.1. Case Study of $\{\Delta r\}^2$. For the case of the fixed tube, the primitive chains at the times t and 0 are mutually overlapping in the portion of the tube surviving at t; see the dashed and solid curves in Figure 1, parts a and b. At these times, the same number ($N\varphi$) of the primitive segments are contained in this portion having the survival fraction φ. Under this situation, the chain conformations at the times 0 and t are characterized by the numbers m_0 and m of the primitive segments out of the left edge of that portion at these times. The m and m_0 values have a distribution in a range between 0 and $N(1-\varphi)$.

In parts a and b of Figure 1, the nth primitive segment is shown with the unfilled circle (with the index n being defined with respect to the left end of the chain). The displacement vector $\Delta\boldsymbol{r}(n,t)$ of this segment is geometrically determined by the m, m_0, and n values. For t well below the terminal viscoelastic relaxation time τ_G, the Fickian diffusion of the chain is negligible and the average of $\{\Delta r\}^2$ is classified into some cases explained below.

Case 1. For $0 \le n < m$ and $0 \le n < m_0$, the nth primitive segment is out of the left edge of the surviving portion of the tube at both times 0 and t. Then, $\Delta\boldsymbol{r}$ is given by $\boldsymbol{r}-\boldsymbol{r}_0$, where $\boldsymbol{r}$ and $\boldsymbol{r}_0$ are the vectors connecting the center of the tube edge and the segment at these times; see Figure 1b. Because of the Gaussian feature of the chains, the $\boldsymbol{r}$ and $\boldsymbol{r}_0$ for the sequences of $m-n$ and m_0-n segments are uncorrelated with each other. Thus, $\Delta\boldsymbol{r}$ is equivalent to an end-to-end vector of a hypothetical Gaussian subchain composed of $m+m_0-2n$ segments, and the *conditional* average of $\{\Delta r\}^2$ evaluated for all conformations of this subchain under a constraint of the *fixed* m, m_0, and n values is written as

$$\overline{[\{\Delta r\}^2]}_{\text{case1}} = a^2(m + m_0 - 2n) \tag{3}$$

Case 2. For $m + N\varphi < n \le N$ and $m_0 + N\varphi < n \le N$, the nth primitive segment is out of the right edge of the surviving portion of the tube at both times 0 and t. This situation is equivalent to that in case 1, and the conditional average of $\{\Delta r\}^2$ is found to be

$$\overline{[\{\Delta r\}^2]}_{\text{case2}} = a^2(2n - m - m_0 - 2N\varphi) \tag{4}$$

Case 3. For $m \le n \le m + N\varphi$ and $m_0 \le n \le m_0 + N\varphi$, the nth primitive segment is in the surviving portion of the tube at both times 0 and t. Then, $\Delta\boldsymbol{r}$ is equivalent to an end-to-end vector $\boldsymbol{\xi}$ of a portion of the chain composed of $|m - m_0|$ segments (see Figure 1a), and the conditional average of $\{\Delta r\}^2$ is given by

$$\overline{[\{\Delta r\}^2]}_{\text{case3}} = a^2|m - m_0| \tag{5}$$

Case 4. For the remaining sets of the m, m_0, and n values, the nth primitive segment is in the surviving portion of the tube at one of the times 0 and t and out of this portion at the other time. A simple geometrical consideration gives the conditional average of $\{\Delta r\}^2$. For example, for $n < m$ and $m_0 < n < m_0 + N\varphi$, $\Delta\boldsymbol{r}$ is given by a difference of the end-to-end vectors of two sequences composed of $m - n$ segments (at time t) and $n - m_0$ segments (at time 0), with both vectors starting from the center of the left edge of the surviving portion of the tube. This $\Delta\boldsymbol{r}$ is equivalent to an end-to-end vector of a hypothetical Gaussian subchain composed of $m - m_0$ segments, and the conditional average $\overline{\{\Delta r\}^2}$ is given by $a^2(m - m_0)$. From a similar consideration for all values of m, m_0, n in case 4, we find

$$\overline{[\{\Delta r\}^2]}_{\text{case4}} = a^2|m - m_0| \tag{6}$$

3.2. Expression of $[d(n,t)]^2$. In general, the equilibrium chain motion is statistically symmetric on reversal of the time (from t to $-t$) and invariant with a shift of the origin of the time. Thus, for a given survival fraction of the fixed tube, φ, the distribution of m and m_0 should be described by a common, normalized distribution function Ψ defined for $0 \le m, m_0 \le N(1-\varphi)$. Utilizing this Ψ, we can express the mean-square displacement (eq 2) as

$$[d(n,t)]^2 = \int_0^{N(1-\varphi)} \mathrm{d}m \int_0^{N(1-\varphi)} \mathrm{d}m_0\, \Psi(m)\Psi(m_0)\, \overline{\{\Delta r(m,m_0,n)\}^2} \tag{7}$$

where $\overline{\{\Delta r\}^2}$ represents the conditional averages for cases 1−4 explained earlier. Among the four cases, more than two cases may emerge for different m and/or m_0 values in the integration range in eq 7, and the $\overline{\{\Delta r\}^2}$ is chosen from those given by eqs 3−6 according to the n, m, and m_0 values.

The $[d(n,t)]^2$ can be unequivocally calculated if the functional form of $\Psi(m)$ is known. However, before considering this form, we examine special cases where $[d(n,t)]^2$ can be deduced from eq 7 without a detailed knowledge about $\Psi(m)$.

3.3. d^2 for End Segment. Only case 1 or case 2 is allowed for the primitive segments at the chain ends ($n = 0$ and N). For these segments, eq 7 is simplified as $[d(0,t)]^2 = a^2\{\langle m\rangle + \langle m_0\rangle\}$ and $[d(N,t)]^2 = a^2\{2N(1-\varphi) - \langle m\rangle - \langle m_0\rangle\}$ with $\langle m\rangle = \langle m_0\rangle = \int_0^{N(1-\varphi)} m\Psi(m)\,\mathrm{d}m$. Since the two ends of the chains are equivalent, the chain should have, on average, the same number of the segments out of the left and right edges of the surviving portion of the tube. Thus, irrespective of the details of

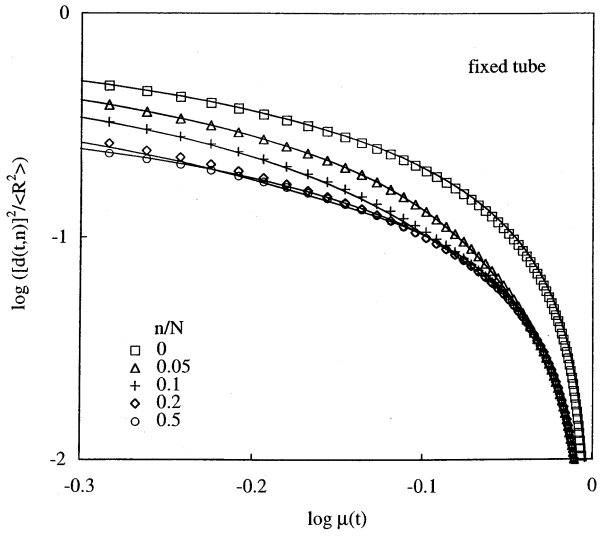

Figure 2. Plots of the normalized mean-square displacement of the nth primitive segment $[d(n,t)]^2/\langle R^2\rangle$ against the normalized viscoelastic relaxation function $\mu(t)$ for the chain in the fixed tube. The $[d(n,t)]^2$ does not include a contribution from the nondiffusive part of CLF. The curves indicate the relationship between d^2 and μ derived in this study (eq 16). The symbols are the plots for the chain reptating in the fixed tube.

$\Psi(m)$, the average number is given by $\langle m\rangle = \langle m_0\rangle = N(1 - \varphi)/2$. (Note that $N(1 - \varphi)$ is the total number of the primitive segments out of that portion.) From this result, we obtain

$$d^2 = \langle R^2\rangle\{1-\varphi(t)\} \quad \text{for the end segments} \qquad (8)$$

Here, $\langle R^2\rangle$ ($= Na^2$) is the mean-square end-to-end distance of the chain.

It should be emphasized that eq 8 was derived without any assumption about the chain motion between the times 0 and t. Thus, eq 8 is generally valid for the chain in the fixed tube in a rather wide range of t where d^2 is negligibly contributed from the Fickian diffusion of the chain.

Equation 8 is valid even if the chains in the system have a distribution in their tube survival fraction: For this case, the φ in eq 8 represents the survival fraction averaged over the chains.

3.4. d^2 for the Middle Segment. For the primitive segment at the middle of the chain ($n = N/2$), all four cases, 1−4, are allowed in the integration range in eq 7 if φ is smaller than 0.5. Thus, for $\varphi < 0.5$, the calculation of d^2 requires detailed information about $\Psi(m)$.

In contrast, for $\varphi > 0.5$, only case 3 is allowed, and eq 7 is reduced to

$$[d(N/2,t)]^2 = a^2\langle|m - m_0|\rangle \qquad (9)$$

with

$$\langle|m - m_0|\rangle = \int_0^{N(1-\varphi)} \mathrm{d}m \int_0^{N(1-\varphi)} \mathrm{d}m_0\, |m - m_0|\Psi(m)\,\Psi(m_0) \qquad (10)$$

Since the variable $|m - m_0|$ appearing in eqs 9 and 10 is equivalent to an absolute value of the curvilinear displacement along the fixed tube, the average $\langle|m - m_0|\rangle$ corresponds to the abandoned number of the initial tube segments at the left (or right) side of the surviving portion of the tube. Thus, this average can be safely approximated as $\langle|m - m_0|\rangle \cong N(1 - \varphi)/2$, and eq 9 is rewritten as

$$d^2 \cong \langle R^2\rangle\{1-\varphi(t)\}/2 \quad \text{for the middle segment } (\varphi > 0.5) \qquad (11)$$

(In fact, for the chain reptating in the fixed tube, d^2 of the middle segment is excellently described by eq 11, as shown later in Figure 2.)

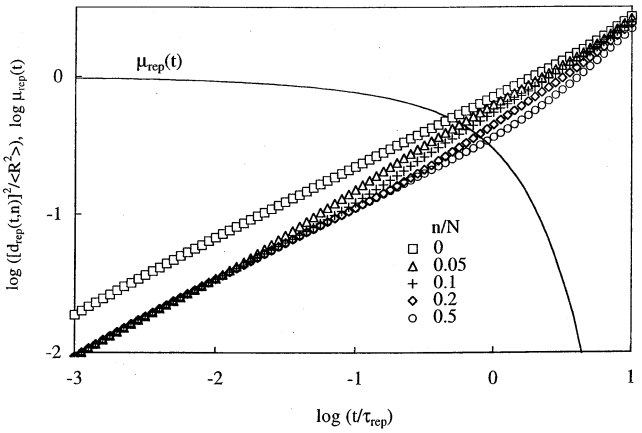

Figure 3. Normalized mean-square displacement of the nth primitive segment $[d_{rep}(n,t)]^2/\langle R^2\rangle$ (symbols) and the normalized viscoelastic relaxation function $\mu_{rep}(t)$ (curve) for the chain reptating in the fixed tube. The $[d_{rep}(n,t)]^2/\langle R^2\rangle$ and $\mu_{rep}(t)$ are plotted against the reduced time, t/τ_{rep}.

For the well-entangled monodisperse linear chains, the range of $\varphi(t) > 0.5$ corresponds to a considerably wide range of t: For example, $\varphi(t) > 0.5$ at $t < 0.5\tau_G$ for the chain reptating in the fixed tube (cf. Figure 3 shown later). For the actual linear PI chains having the type-A dipoles, the DTD picture is valid at long t and the survival fraction of the dilated tube $\varphi'(t)$ is very close to the dielectric relaxation function $\Phi(t)$.[8,11,12] This $\varphi'(t)$, playing a role analogous to $\varphi(t)$ of the fixed tube, is also larger than 0.5 in a wide range of $t < 0.5\tau_G$; cf. Figure 15 in ref 12 (with the dielectric τ_ϵ shown therein being close to $2\tau_G$).

Thus, the analysis of d^2 in a range of $\varphi > 0.5$ (and $\varphi' > 0.5$) is sufficient for our aim of testing the DTD picture at *short t* well below τ_G. For this reason, the analysis in the remaining part of this paper is limited only in a range of φ and φ' being larger than 0.5. In fact, the prerequisite of our analysis, negligible Fickian diffusion of the chain, is fulfilled in this range; cf. Figure 3 shown later.

3.5. d^2 for $0 \le n \le N$. For $\varphi(t) > 0.5$, the $[d(n,t)]^2$ calculated from eq 7 is classified into three regimes specified below according to the n value.

Regime i. $0 \le n < N(1 - \varphi)$

$$\left\{\frac{d(n,t)}{a}\right\}^2 = \langle|m - m_0|\rangle + \mathrm{I} \qquad (12a)$$

with

$$\mathrm{I} = \int_n^{N(1-\varphi)} \mathrm{d}m \int_n^{N(1-\varphi)} \mathrm{d}m_0\,\{m+m_0 - 2n - |m - m_0|\}\Psi(m)\Psi(m_0) \qquad (12b)$$

Regime ii. $N(1 - \varphi) \le n \le N\varphi$

$$\left\{\frac{d(n,t)}{a}\right\}^2 = \langle|m - m_0|\rangle \qquad (13)$$

Regime iii. $N\varphi < n \leq N$

$$\left\{\frac{d(n,t)}{a}\right\}^2 = \langle|m - m_0|\rangle + \mathrm{III} \tag{14a}$$

with

$$\mathrm{III} = \int_0^{n-N\varphi} \mathrm{d}m \int_0^{n-N\varphi} \mathrm{d}m_0 \{2n\text{-}2N\varphi - m - m_0 - |m - m_0|\}\Psi(m)\Psi(m_0) \tag{14b}$$

Here, the average $\langle|m - m_0|\rangle$ is defined by eq 10: As explained earlier, this average can be approximated as $\langle|m - m_0|\rangle \cong N(1 - \varphi)/2$.

The integrals I and III can be accurately evaluated only when $\Psi(m)$ is explicitly known. However, the number m of the primitive segments out of the left edge of the surviving portion of the tube would have a broad distribution and $\Psi(m)$ would be rather weakly dependent on m. Considering this qualitative feature of $\Psi(m)$ and the width of the integration ranges in eqs 12b and 14b, we attempted to approximate the integrals as

$$\mathrm{I} \cong \left\{\frac{N(1 - \varphi)\text{-}n}{N(1 - \varphi)}\right\}^2 [\langle m + m_0 - |m - m_0|\rangle - n] \tag{15a}$$

$$\mathrm{III} \cong \left\{\frac{n\text{-}N\varphi}{N(1 - \varphi)}\right\}^2 [n + N - 2N\varphi - \langle m + m_0 + |m - m_0|\rangle] \tag{15b}$$

Here, the average $\langle\cdots\rangle$ is taken in the entire range of $0 < m, m_0 < N(1 - \varphi)$. This approximation may look very crude. However, the d^2 calculated with this approximation is surprisingly close to that of the chain reptating in the fixed tube, as shown later in Figure 2.

Equations 12−15 specify the n dependence of $[d(n,t)]^2$ in the range of $\varphi(t) > 0.5$ and at t longer than τ_{Rouse}. Now, we cast eqs 12−15 into a relationship between experimentally measurable quantities, d^2 and the normalized viscoelastic relaxation function $\mu(t)$. For the chain in the fixed tube, $\mu(t)$ coincides with $\varphi(t)$. Thus, d^2 given by eqs 12−15 is expressed in terms of μ as

$$d^2 \cong \langle R^2\rangle\left[\frac{1 - \mu}{2} + \left(1 - \frac{\theta}{1 - \mu}\right)^2\left\{\frac{1 - \mu}{2} - \theta\right\}\right] \quad \text{for } 0 \leq \theta \leq 1 - \mu \tag{16a}$$

$$d^2 \cong \langle R^2\rangle\left(\frac{1 - \mu}{2}\right) \quad \text{for } 1 - \mu < \theta < \mu \tag{16b}$$

$$d^2 \cong \langle R^2\rangle\left[\frac{1 - \mu}{2} + \left(\frac{\theta - \mu}{1 - \mu}\right)^2\left\{\theta - \frac{1 + \mu}{2}\right\}\right] \quad \text{for } \mu \leq \theta \leq 1 \tag{16c}$$

Here, $\theta = n/N$ is the reduced index of the primitive segment.

A few comments need to be added for the above results. First of all, the d^2 given by eq 16 is symmetric with respect to the chain center ($[d(n,t)]^2 = [d(N - n,t)]^2$), as naturally expected from the equivalence of the two ends of the chain. More importantly, eq 16 with $\theta = 0$ and 1 is reduced to eq 8, the expression of d^2 for the end segment derived with no approximation.

3.6. Accuracy of eq 16. For $\mu > 0.5$ ($\varphi > 0.5$), the dependence of d^2 on μ (eq 16) is shown in Figure 2 with the curves. The reduced index of the primitive segment, n/N, is 0, 0.05, 0.1, 0.2, and 0.5 from the top to bottom. In this range of μ, the segments near the center of the chain have almost identical d^2 (because the curvilinear motion along the tube dominates the d^2; cf. Figure 1a) while the segments near the chain end exhibit larger d^2 (due to the motion in a free space out of the surviving portion of the tube; cf. Figure 1b).

To examine the numerical accuracy of our analysis, we compared the d^2 given by eq 16 with the $d_{\mathrm{rep}}{}^2$ of a chain reptating in the fixed tube. For this chain, $d_{\mathrm{rep}}{}^2$ and μ_{rep} are explicitly calculated as functions of t,[3,7]

$$[d_{\mathrm{rep}}(n,t)]^2 = \langle R^2\rangle\left[\frac{2}{\pi^2}\left(\frac{t}{\tau_{\mathrm{rep}}}\right) + \sum_{p=1}^{\infty}\frac{4}{p^2\pi^2}\cos^2\left(\frac{p\pi n}{N}\right)\left\{1 - \exp\left(-\frac{p^2 t}{\tau_{\mathrm{rep}}}\right)\right\}\right] \tag{17}$$

$$\mu_{\mathrm{rep}}(t) = \sum_{p=\mathrm{odd}}\frac{8}{p^2\pi^2}\exp\left(-\frac{p^2 t}{\tau_{\mathrm{rep}}}\right) \tag{18}$$

Here, τ_{rep} is the reptation time. In Figure 3, $d_{\mathrm{rep}}{}^2$ and μ_{rep} are plotted against t/τ_{rep}. From these plots, we note that the range of $\mu_{\mathrm{rep}} > 0.5$ ($\varphi > 0.5$) corresponds to the range of $t < 0.5\tau_{\mathrm{rep}}$. We also note that the Fickian diffusion, being represented by the $2t/\pi^2\tau_{\mathrm{rep}}$ term in eq 17 and characterized by the proportionality between d^2 and t, does not significantly contribute to the d^2 in this range of μ_{rep}.

In Figure 2, the plots of $d_{\mathrm{rep}}{}^2$ against μ_{rep} are shown with the symbols. The curves obtained from our analysis (eq 16) agree with the plots very well. The top curve for the end segment was obtained from the general consideration (cf. eq 8), and the excellent agreement between this curve and the plot (square) is naturally expected. More importantly, the bottom curve for the middle segment obtained under the approximation ($\langle|m - m_0|\rangle \cong N(1 - \varphi)/2$; cf. eq 11) agrees with the plot (circle), indicating the validity of this approximation. Furthermore, the remaining curves for the segments having $0 < n < N/2$ are also close to the plots, suggesting the acceptable accuracy of the approximation (eq 15) utilized for obtaining those curves.

Thus, for the chain in the fixed tube, eq 16 describes the relationship between d^2 and μ (>0.5) with satisfactory accuracy. This result allows us to utilize eq 16 to derive the relationship for the chain in the dilated tube.

4. Relationship between d^2 and μ for the Chain in Dilated Tube

Here, we consider the primitive chain in the fully dilated tube having the survival fraction $\varphi'(t)$ and the diameter $a' = a\{\varphi'(t)\}^{-\alpha/2}$ ($\alpha = 1$−1.3). In Figure 1, parts c and d, this chain at the times 0 and t is shown with the dashed and solid curves. The number of the primitive segments in the surviving portion of the dilated tube is given by $N\varphi'(t)$.

In the range of $\varphi'(t) > 0.5$, we utilized eq 16 (for the case of the fixed tube) to calculate the $[d(n,t)]^2$ of the chain in the dilated tube. The results are summarized below.

4.1. Evaluation of $\overline{\{\Delta r\}^2}$. As in the case of the fixed tube, the chain conformations at the times 0 and t are characterized by the numbers m_0 and m of the primitive segments out of the left edge of the surviving portion of the dilated tube; see Figure 1, parts c and d. However, differing from that case, the primitive chains at these

times are not superimposed with each other even at their portions contained in the surviving part of the dilated tube. This lack of superposition results from the lateral motion in the dilated tube that occurs in the interval of time between 0 to t. For this case, we can evaluate the displacement vector $\Delta\boldsymbol{r}(n,t)$ of the nth segment (unfilled circle) by hypothetically dividing the chain motion in two steps, as explained below.

In step 1, the chain is regarded to move in a fixed tube hypothetically considered around the chain at the time 0. The number of the primitive segments contained in this tube at the time t is identical to that in the dilated tube ($=N\varphi'$), and the survival fraction of the hypothetical fixed tube at t is given by φ'. The displacement vector $\Delta\boldsymbol{r}_{(1)}$ in step 1 is equivalent to those explained for eqs 3−6. For example, if the nth segment is out of the surviving portion of the fixed tube in the two states before and after step 1, $\Delta\boldsymbol{r}_{(1)}$ is given by a difference of the vectors $\boldsymbol{r}$ and $\boldsymbol{r}_0$ connecting the edge of this portion and the segment positions in these states (cf. Figure 1, parts a and b). For the other case that the nth segment is in the surviving portion at those states, $\Delta\boldsymbol{r}_{(1)}$ coincides with an end-to-end vector $\boldsymbol{\xi}$ of a Gaussian sequence of $|m - m_0|$ segments (cf. Figure 1, parts a and c; the dotted circle in Figure 1c indicates the location of the segment after step 1).

In step 2 following step 1, the chain is considered to laterally fluctuate in the dilated tube without exhibiting the longitudinal motion. If the nth primitive segment is in the surviving portion of the dilated tube after step 1, the $\Delta\boldsymbol{r}_{(2)}$ for step 2 coincides with a displacement $\boldsymbol{D}$ of this segment in an internal cross section of this portion (shown with the dotted ellipse in Figure 1c). For the other cases, $\Delta\boldsymbol{r}_{(2)}$ is given by a displacement $\boldsymbol{D}$ of a segment located at the edge of the surviving portion; cf. small filled circles shown in Figure 1d. In general, this edge segment is not the same segment at the time 0 (before step 1) and the time t (after step 2) because of the longitudinal motion during step 1:[12] $\boldsymbol{D}$ is defined as a vector connecting the positions of the edge segment at these times.

In the actual situation, the chain should exhibit the longitudinal and lateral movements simultaneously. However, the net displacement of the nth primitive segment $\Delta\boldsymbol{r}$ coincides with a sum of the $\Delta\boldsymbol{r}_{(1)}$ and $\boldsymbol{D}$ for the above hypothetical steps. Two lateral displacements in the opposite directions, $\boldsymbol{D}$ and $-\boldsymbol{D}$, occur with the same probability for a given $\Delta\boldsymbol{r}_{(1)}$, and $\Delta\boldsymbol{r}_{(1)}$ and $\boldsymbol{D}$ are not correlated with each other. Thus, the conditional average of $\{\Delta r\}^2$ for the given m, m_0, and n values is obtained as

$$\overline{\{\Delta r\}^2} = \overline{\{\Delta r_{(1)}\}^2} + \langle D^2\rangle \tag{19}$$

Here, $\overline{\{\Delta r_{(1)}\}^2}$ is given by one of eqs 3−6 according to the m, m_0, and n values. The average $\langle D^2\rangle$ is calculated from the distribution of the lateral displacement that is determined by the dilated tube diameter a' (and independent of the m, m_0, and n values).

If the nth primitive segment is in the surviving portion of the dilated tube after step 1 (Figure 1c), the segment position in the two states after steps 1 and 2 should be uniformly distributed in the internal cross section of this tube (shown with the dotted ellipse). Then, $\boldsymbol{D}$ is equivalent to a vector connecting arbitrary chosen two points in a circular region of the diameter $a' - a$, the region available for the center of the nth segment. This equivalence holds also for the other cases where $\boldsymbol{D}$ represents the random displacement of the edge segment.[12] Thus, for all cases, $\langle D^2\rangle$ can be evaluated as[12,16]

$$\langle D^2\rangle = \frac{1}{\pi^2\{(a'-a)/2\}^4}\int\{(x - x_0)^2 + (y - y_0)^2\}\,dx\,dx_0\,dy\,dy_0$$

$$= \frac{a^2}{4}[\{\varphi'(t)\}^{-\alpha/2} - 1]^2 \tag{20}$$

Here, (x_0, y_0) and (x, y) are the coordinates of the two points explained above, and the integral is conducted in a range of $(x_0^2 + y_0^2) < (a' - a)^2/4$ and $(x^2 + y^2) < (a' - a)^2/4$. (The DTD relationship, $a' = a\{\varphi'(t)\}^{-\alpha/2}$, has been utilized in eq 20.)

4.2. Expression of d^2. The mean-square displacement $[d(n,t)]^2$ for the case of DTD (with $\varphi' > 0.5$) can be obtained by inserting eq 19 into eq 7. The $\langle D^2\rangle$ term in eq 19 is independent of m and m_0 and the contribution of this term to d^2 is given by $(a^2/4)(\varphi'^{-\alpha/2} - 1)^2$ (eq 20). The $\overline{\{\Delta r_{(1)}\}^2}$ term, due to the motion of the chain in the fixed tube having the survival fraction φ' at t (step 1), is equivalent to the conditional averages given by eqs 3−6. Thus, the contribution of the $\overline{\{\Delta r_{(1)}\}^2}$ term to d^2 is given by eqs 12−15 with φ being replaced by φ'. (Correspondingly, the averages included in eqs 12−15 are replaced by $\langle|m - m_0|\rangle \cong N(1 - \varphi')/2$ and $\langle m\rangle = \langle m_0\rangle = N(1 - \varphi')/2$.)

Now, we express $\varphi'(t)$ in terms of the experimentally measurable $\mu(t)$; $\varphi'(t) = [\mu(t)]^\delta$ with $\delta = 1/(1 + \alpha) \cong {}^1/_2$ for the case of DTD.[1−5] Replacing the φ' in the above contributions of the $\langle D^2\rangle$ and $\overline{\{\Delta r_{(1)}\}^2}$ terms by μ^δ, we finally obtain

$$d^2 \cong \langle R^2\rangle\left[\frac{1 - \mu^\delta}{2} + \left(1 - \frac{\theta}{1 - \mu^\delta}\right)^2\left(\frac{1 - \mu^\delta}{2} - \theta\right) + \frac{1}{4N}(\mu^{-\alpha\delta/2} - 1)^2\right] \quad \text{for } 0 \le \theta < 1 - \mu \tag{21a}$$

$$d^2 \cong \langle R^2\rangle\left[\frac{1 - \mu^\delta}{2} + \frac{1}{4N}(\mu^{-\alpha\delta/2} - 1)^2\right] \quad \text{for } 1 - \mu \le \theta \le \mu \tag{21b}$$

$$d^2 \cong \langle R^2\rangle\left[\frac{1 - \mu^\delta}{2} + \left(\frac{\theta - \mu^\delta}{1 - \mu^\delta}\right)^2\left(\theta - \frac{1 + \mu^\delta}{2}\right) + \frac{1}{4N}(\mu^{-\alpha\delta/2} - 1)^2\right] \quad \text{for } \mu < \theta \le 1 \tag{21c}$$

with $\theta = n/N$. This d^2 is symmetric with respect to the chain center ($[d(n,t)]^2 = [d(N - n,t)]^2$).

Equation 21 was derived from the consideration about the Gaussian feature of the chain, and the approximation utilized in this derivation is the same as the approximation underlying eq 16 for the case of the fixed tube. As judged from the success of eq 16 for the chain reptating in the fixed tube (Figure 2), eq 21 should satisfactorily describe the actual d^2 data whenever the DTD picture is valid (i.e., irrespective of the details of the chain motion). Thus, eq 21 provides us with a reliable basis for the test of this picture at short t where $\varphi' = \mu^\delta > 0.5$.

Specifically, the relationship for the primitive segment at the chain ends, eq 21 with $\theta = 0$ and 1, is derived

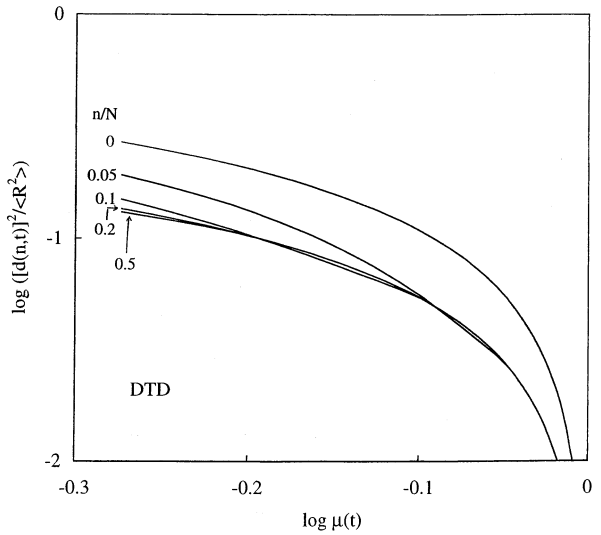

Figure 4. Relationship between the normalized mean-square displacement of the nth primitive segment $[d(n,t)]^2/\langle R^2\rangle$ and the normalized viscoelastic relaxation function $\mu(t)$ derived for the chain in the dilated tube (eq 21). The $[d(n,t)]^2$ does not include a contribution from the nondiffusive part of CLF.

with no approximation and is valid irrespective of the distribution of the tube survival fraction among the chains (as similar to the situation explained for eq 8). Thus, this relationship would serve as the most reliable basis for the test of the DTD picture.

In Figure 4, the d^2 given by eq 21 with $\delta = {}^1/_2$ and $\alpha = 1$ are plotted against μ. The number of the primitive segments per chain is $N = 50$ (in the highly entangled regime), and the reduced segment index n/N is 0, 0.05, 0.1, 0.2, and 0.5 from the top to bottom. For this N value, the d^2 in the range of $\mu > 0.5$ was negligibly contributed from the $(\mu^{-\alpha\delta/2} - 1)^2/4N$ term in eq 21 (representing the lateral motion in the dilated tube). This was the case for all N values > 10 and $\mu > 0.5$.

As seen in Figure 4, the primitive segments near the center of the chain have almost identical d^2 while the segments near the chain end exhibit larger d^2. This feature of d^2 is qualitatively similar to that for the case of the fixed tube (Figure 2). However, we also note a quantitative difference: The d^2 for a given value of μ is considerably smaller, by a factor $\cong 1.8$, for the DTD case (Figure 4) than for the non-DTD case (Figure 2). This difference does *not* mean that the segmental displacement is slower for the case of DTD. Instead, it reflects a fact that the DTD hardly affects the segmental displacement at short t (as noted from the negligible contribution of the lateral motion term explained above) but significantly accelerates the viscoelastic relaxation.

5. Experimental Mode of the Test of DTD Picture at Short *t*

5.1. Evaluation of d^2 at Short t. Here, we focus on a real (nonprimitive) chain composed of gN monomeric segments, with g being the number of these segments per primitive segment. The Rouse segment having the Kuhn molecular weight, utilized as the minimum motional unit of flexible chains,[13,14] is chosen as this monomeric segment. The mean-square displacement of the jth monomeric segment is defined as $[\delta(j,t)]^2 = \langle[\Delta\boldsymbol{\rho}(j,t)]^2\rangle$, where $\Delta\boldsymbol{\rho}(j,t)$ is the displacement vector of this segment in an interval of time between 0 to t. If this monomeric segment is appropriately labeled (with an isotope and/or a dye, for example), its δ^2 can be measured from a variety of experiments such as diffusion experiments utilizing the forward recoil spectrometry[17] and dynamic scattering[18] experiments.

The mean-square displacement of the nth primitive segment $[\mathscr{D}(n,t)]^2$ is defined as $\langle[\Delta\boldsymbol{\rho}_{CM}(t)]^2\rangle$, where $\Delta\boldsymbol{\rho}_{CM}(t)$ is a displacement vector of the center of mass (CM) of the g monomeric segments included in this primitive segment. In the range of t considered in this paper ($\tau_{Rouse} < t < 0.5\tau_G$), these monomeric segments are mutually equilibrated and their displacement vector is given by $\Delta\boldsymbol{\rho}(j,t) = \Delta\boldsymbol{\rho}_{CM}(t) + \Delta\boldsymbol{\rho}_f(j,t)$, where $\Delta\boldsymbol{\rho}_f(j,t)$ represents the random fluctuation of the jth monomeric segment around CM. Since $\Delta\rho_{CM}(t)$ and $\Delta\rho_f(j,t)$ are not correlated with each other, $[\mathscr{D}(n,t)]^2$ is written as

$$[\mathscr{D}(n,t)]^2 = [\delta(j,t)]^2 - \delta_f^2 \quad \text{with } \delta_f^2 = \langle[\Delta\boldsymbol{\rho}_f(j,t)]^2\rangle \quad (\text{for } \tau_{Rouse} < t < 0.5\tau_G) \quad (22)$$

The δ_f^2 term in eq 22 is independent of t, j, and n, because the fluctuation around CM at $t > \tau_{Rouse}$ is equivalent to full randomization of the monomeric segment position within the primitive segment.

The δ_f^2 has a value of $O(a^2)$. Since the monomeric segment is much smaller than the primitive segment, we may approximate δ_f^2 as a mean-square separation of two points randomly chosen in a sphere of the diameter a. Then, δ_f^2 is calculated to be

$$\delta_f^2 = \frac{1}{\{4\pi(a/2)^3/3\}^2}\int\{(x-x_0)^2 + (y-y_0)^2 + (z-z_0)^2\}\,dx\,dx_0\,dy\,dy_0\,dz\,dz_0$$

$$= \frac{3}{10}a^2 \quad (23)$$

Here, (x_0, y_0, z_0) and (x, y, z) are the coordinates of the two points explained above, and the integral is conducted in the sphere of the diameter a.

The $[\mathscr{D}(n,t)]^2$ of the nth primitive segment can be evaluated by subtracting this δ_f^2 from the $[\delta(j,t)]^2$ data of a monomeric segment included in this primitive segment. In practice, we should utilize an average $[\delta_{av}(n,t)]^2 = (1/g)\sum_j [\delta(j,t)]^2$ taken for all g monomeric segments in the primitive segment, instead of $[\delta(j,t)]^2$ of one monomeric segment, to enhance the accuracy of the evaluated $[\mathscr{D}(n,t)]^2$. This $[\delta_{av}(n,t)]^2$ can be directly measured for the *partially labeled* chain having the appropriate label on these g segments: cf. Appendix for the dynamic scattering measurement.

The quantity required for the test of eqs 16 and 21, $[d(n,t)]^2$, is the mean-square displacement of the nth primitive segment *not* contributed from the a nondiffusive part of the contour length fluctuation (CLF). In the range of $\tau_{Rouse} < t < 0.5\tau_G$ (where $\mu(t) > 0.5$), this $[d(n,t)]^2$ is given by $[\mathscr{D}(n,t)]^2 - d_{CLF}^2$ with d_{CLF}^2 being the mean-square displacement due only to the nondiffusive part of CLF. This d_{CLF}^2 is independent of t and n at $t > \tau_{Rouse}$ where the CLF process is completed.

The d_{CLF}^2 has a value of $O(a^2N^{1/2})$ at $t > \tau_{Rouse}$.[7] This value can be calculated from an expression of $[d_{CLF}(n,t)]^2$ for the nondiffusive part of the Rouse-type CLF process as[7]

$$[d_{\mathrm{CLF}}(n,t)]^2 = a^2N^{1/2}\left[\sum_{p=1}^{\infty}\frac{4}{3p^2\pi^2}\cos^2\left(\frac{p\pi n}{N}\right)\left\{1-\exp\left(-\frac{p^2t}{\tau_{\mathrm{Rouse}}}\right)\right\}\right]^{1/2} \rightarrow a^2N^{1/2}/3 \text{ for } t > \tau_{\mathrm{Rouse}} \quad (24)$$

In this calculation, the exponential terms were approximated to be zero at $t > \tau_{\mathrm{Rouse}}$, and the $\cos^2(p\pi n/N)$ terms were replaced by their average, $^1/_2$.[7]

Thus, the $[d(n,t)]^2$ required for our test of the DTD picture is evaluated from the measured $[\delta_{\mathrm{av}}(n,t)]^2$ data as

$$[d(n,t)]^2 = [\delta_{\mathrm{av}}(n,t)]^2 - {\delta_{\mathrm{f}}}^2 - {d_{\mathrm{CLF}}}^2 \quad (25)$$

with $\delta_{\mathrm{f}}^2 \cong 3a^2/10$ and $d_{\mathrm{CLF}}^2 \cong a^2N^{1/2}/3$.

Here, we note that the approximations in the calculation of δ_{f}^2 (eq 23) and d_{CLF}^2 (eq 24) may introduce some uncertainty in the test made for this $[d(n,t)]^2$. To avoid this uncertainty, we can consider a general feature that δ_{f}^2 and d_{CLF}^2 are independent of n and t at $t > \tau_{\mathrm{Rouse}}$ and focus on a difference of the displacements of two primitive segments

$$\Delta(n,n',t) = [d(n,t)]^2 - [d(n',t)]^2 = [\delta_{\mathrm{av}}(n,t)]^2 - [\delta_{\mathrm{av}}(n',t)]^2 \quad (n \neq n') \quad (26)$$

This $\Delta(n,n',t)$ is evaluated, without the calculation of δ_{f}^2 and d_{CLF}^2, directly from the δ_{av}^2 data for two chains labeled at the nth and n'th primitive segments. Thus, the DTD picture at short t can be most reliably tested for $\Delta(n,n',t)$.

5.2. Test of DTD picture at Short *t*. As explained in the Introduction, the μ data are satisfactorily obtained by subtracting a contribution of the fast, local relaxation processes from the measured relaxation modulus with the aid of the modified stress−optical rule. Furthermore, for highly entangled linear chains, the contribution of the fast processes is negligible and the measured modulus is equivalent to $\mu(t)$ in a dominant part in the range of $\tau_{\mathrm{Rouse}} < t < 0.5\tau_{\mathrm{G}}$.

Since eqs 16 and 21 give significantly different values of $[d(n,t)]^2$ and/or $\Delta(n,n',t)$ $(= [d(n,t)]^2 - [d(n',t)]^2;\ n \neq n')$, we can unambiguously test the DTD picture at short t by comparing the μ data with the d^2 and Δ data, the latter two being obtained from the mean-square displacement δ_{av}^2 measured for the partially labeled chains (cf. eqs 25 and 26): Those data should obey eq 21 if this picture is valid and the tube actually dilates to the diameter $a' = a\{\mu(t)\}^{-\alpha\delta/2}$ $(=a\{\varphi'(t)\}^{-\alpha/2})$, while eq 16 should be satisfied if the tube does not dilate in a range of t examined. If the tube dilates just *insufficiently* (to a diameter smaller than $a\{\mu(t)\}^{-\alpha\delta/2}$), the d^2 and Δ data would be between those calculated from eqs 16 and 21.

The above test is made most reliably for the $\mu(t)$ and $\Delta(n,n',t)$ data, because the evaluation of the latter requires no approximate calculation of δ_{f}^2 and d_{CLF}^2 (eqs 23 and 24). In the entire range of n and n', Δ has the maximum value at $n = 0$ and $n' = N/2$; cf. Figures 2 and 4. Thus, the test would be most successfully achieved for the $\Delta(0,N/2,t)$ data. (Namely, experiments would most clearly distinguish the non-DTD and DTD relationships (eqs 16 and 21) for $\Delta(0,N/2,t)$.)

The test may be satisfactorily made also for the μ and d^2 data when the measured δ_{av}^2 is not very close to the calculated sum $\delta f^2 + d_{\mathrm{CLF}}^2$ $(=a^2N^{1/2}/3 = \langle R^2\rangle/3N^{1/2}$ for $N \gg 1)$ and the d^2 obtained after the subtraction of this sum (eq 25) is not smaller than the sum. Thus, the test is most easily made for the end segment having the largest d^2 among all segments: For example, $\delta_{\mathrm{f}}^2 + d_{\mathrm{CLF}}^2 = 0.05\langle R^2\rangle$ for a highly entangled chain with $N = 50$, while d^2 of the end segment is larger than this sum at $\mu < 0.9$ (cf. Figures 2 and 4). For this chain, d^2 would be satisfactorily obtained in this range of μ, and the DTD picture can be tested accordingly. (For longer chains, the test can be made even at larger μ.)

The modes of the test explained above require experiments for the partially labeled chains. However, the test can be also made for a fully labeled chain: For this chain, the mean-square displacement averaged for all gN monomeric segments, $\overline{[\delta_{\mathrm{av}}(t)]^2} = (1/gN)\sum_{j=1}^{gN}[\delta(j,t)]^2$ $(=(1/N)\sum_{n=1}^{N}[\delta_{\mathrm{av}}(n,t)]^2)$, can be measured from the diffusion and/or dynamic scattering experiments (see Appendix for the latter). From this $\overline{[\delta_{\mathrm{av}}(t)]^2}$ at $t > \tau_{\mathrm{Rouse}}$, the average of d^2 taken for the N primitive segments of the chain is evaluated as (cf. eq 25)

$$[d_{\mathrm{av}}(t)]^2 = \overline{[\delta_{\mathrm{av}}(t)]^2} - {\delta_{\mathrm{f}}}^2 - {d_{\mathrm{CLF}}}^2 \quad (27)$$

From eqs 16 and 21, $[d_{\mathrm{av}}(t)]^2$ $(=(1/N)\int_0^N [d(n,t)]^2\,\mathrm{d}n$ for $N \gg 1)$ is calculated to be

$$[d_{\mathrm{av}}(t)]^2 = \langle R^2\rangle\left[\frac{1-\mu}{2} + \frac{(1-\mu)^2}{6}\right] \quad \text{for the non-DTD (fixed tube) case} \quad (28)$$

$$[d_{\mathrm{av}}(t)]^2 = \langle R^2\rangle\left[\frac{1-\mu^{\delta}}{2} + \frac{(1-\mu^{\delta})^2}{6} + \frac{(\mu-\mu^{\delta})^3}{(1-\mu^{\delta})^2}\left(\frac{1}{3} + \frac{\mu^{\delta}}{6} - \frac{\mu}{2}\right)\right] \quad \text{for the DTD case} \quad (29)$$

The lateral motion in the dilated tube, represented by the $(\mu^{-\alpha\delta/2} - 1)^2/4N$ term in eq 21, hardly contributes to the $[d(n,t)]^2$ of the well-entangled chains in the range of $\mu > 0.5$, as explained for Figure 4. Thus, this motion has been neglected in eq 29.

In Figure 5, the $[d_{\mathrm{av}}(t)]^2$ given by eqs 28 and 29 (with $\delta = {}^1/_2$) are plotted against μ. The large difference between the $[d_{\mathrm{av}}(t)]^2$ vs μ curves for the non-DTD and DTD cases allows us to test the DTD picture at short t from the simplest experiment for the fully labeled chain (placed in a matrix of unlabeled chains having the same molecular weight). This test can be satisfactorily achieved in a range of μ where the measured $\overline{\{\delta_{\mathrm{av}}(t)\}^2}$ is not very close to the calculated sum $\delta_{\mathrm{f}}^2 + d_{\mathrm{CLF}}^2$, as similar to the situation for the test utilizing $[d(n,t)]^2$.

To our knowledge, no report has been made for the μ, $[\delta_{\mathrm{av}}(n,t)]^2$, and/or $\overline{[\delta_{\mathrm{av}}(t)]^2}$ data measured for the same polymeric system at short t (but still longer than τ_{Rouse}). Thus, the above test cannot be made for the available literature data. This test is considered to be an interesting subject for future work.

Finally, we should emphasize that the DTD picture at short t can be equally examined, *in principle*, through comparison of the viscoelastic μ and dielectric Φ data. (Namely, eq 1 holds in a range of μ where eq 21 is satisfied, and vice versa.) However, for the μ and Φ data, the practical difficulty explained in Introduction disturbs the clear distinction between the DTD and non-DTD cases. No similar difficulty exists in the test

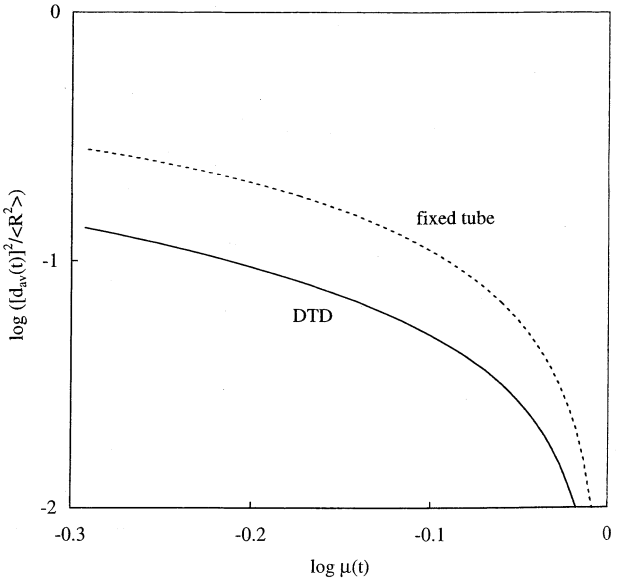

Figure 5. Mean-square displacement averaged for all primitive segments in the chain, $[d_{av}(t)]^2$. This $[d_{av}(t)]^2$ does not include a contribution from the nondiffusive part of CLF. The dotted and solid curves, respectively, indicate $[d_{av}(t)]^2$ for the non-DTD and DTD cases (eqs 28 and 29).

utilizing the segmental displacement instead of Φ, in particular in the test made for μ and Δ.

We should also make a comment for a relationship between $\Phi(t)$ and $[d(n,t)]^2$. For the type-A chain in the fixed and dilated tubes, respectively, $\Phi(t)$ coincides with the tube survival fractions $\varphi(t)$ and $\varphi'(t)$ except for the contribution from the segmental motion in the tube edge.[11,12] At short t examined in this paper, this contribution is negligibly small and the relationship between Φ and d^2 is the *same* for the non-DTD and DTD cases; compare eq 16 (with $\mu = \varphi = \Phi$) and eq 21 (with $\mu^\delta = \varphi' = \Phi$). Namely, the DTD picture at short t can be never tested from the comparison of the Φ and d^2 data. This fact demonstrates the importance of the test made through the comparison of the viscoelastic and segmental displacement data.

6. Concluding Remarks

For well-entangled monodisperse linear chains, we have derived a relationship between the mean-square displacement of the nth primitive segment $[d(n,t)]^2$ (not contributed from the nondiffusive part of CLF) and the normalized viscoelastic relaxation function $\mu(t)$ at short t (but still longer than τ_{Rouse}). This derivation was made by just considering the Gaussian feature of the chain. Specifically, the relationship based on no approximation (and being valid irrespective of the distribution of the tube survival fraction among the chains) was derived for the segment at the chain end.

The relationship thus derived was significantly different for the cases of the absence and presence of DTD: For a given μ (>0.5), d^2 was smaller, by a factor $\cong$1.8, for the DTD case than for the non-DTD case. This result reflects a fact that the DTD hardly affects the segment displacement at short t but significantly accelerates the viscoelastic relaxation. On the basis of this difference, we can test the DTD picture at short t by comparing the μ data with the $[d(n,t)]^2$ and/or $[d(n,t)]^2 - [d(n',t)]^2$ data. This test is considered to be an interesting subject of future work.

Acknowledgment. We thank Professor T. Kanaya at Institute for Chemical Research, Kyoto University, for his invaluable comments. This work was initiated during the stay of H.W. at the Institute for Theoretical Physics, University of California, Santa Barbara. He acknowledges partial support from the National Science Foundation under Grant No. PHY 99-07949 (Reprint No. NSF−ITP-02-178). He also acknowledges partial support from the Ministry of Education, Culture, and Sports, Science, and Technology, Japan under Grant No. 13450391. A.K.R.P. acknowledges, with thanks, financial support from JSPS under its Postdoctoral Research Program (P01279).

Appendix. Determination of Segmental Displacement from Dynamic Scattering Experiments

We consider the chain having the scattering label (such as the isotope label) only on g monomers in the nth primitive segment. For this partially labeled chain (placed in a matrix of unlabeled chains of the same molecular weight), the incoherent intermediate scattering function $I_s(\boldsymbol{q},t)$ at the wave vector $\boldsymbol{q}$ and time t can be written as[18]

$$I_s(\boldsymbol{q},t) = \frac{1}{g}\sum_j \langle \exp\{i\boldsymbol{q}\cdot\Delta\boldsymbol{\rho}(j,t)\}\rangle \quad (i = \sqrt{-1}) \quad \text{(A1)}$$

Here, $\Delta\boldsymbol{\rho}(j,t)$ is the displacement vector of the jth monomeric segment in an interval of time from 0 to t, and the summation $\sum_j$ is taken for the g monomeric segments in the nth primitive segment. (In eq A1, we have coarse-grained all scattering elements (e.g., nuclei for the neutron beam) into one element placed at the center of the labeled monomeric segment. This coarse-graining can be safely made in the range of t ($>\tau_{Rouse}$) considered in this paper.)

Under the Gaussian approximation,[18] this $I_s(\boldsymbol{q},t)$ is rewritten as

$$I_s(\mathbf{q},t) = \frac{1}{g}\sum_j \exp\left(-\frac{q^2}{6}\langle[\Delta\boldsymbol{\rho}(j,t)]^2\rangle\right)$$

$$= 1 - \frac{q^2}{6}\left[\frac{1}{g}\sum_j \langle[\Delta\boldsymbol{\rho}(j,t)]^2\rangle\right] + O(q^4) \quad \text{(A2)}$$

Thus, the mean-square displacement averaged for the g monomeric segments, $[\delta_{av}(n,t)]^2 = (1/g)\sum_j\langle[\Delta\boldsymbol{\rho}(j,t)]^2\rangle$, is evaluated as a slope of the plot of the $1 - I_s(\boldsymbol{q},t)$ data against q^2 in a low-q regime. This $[\delta_{av}(n,t)]^2$ is utilized in eqs 25 and 26 to evaluate $[d(n,t)]^2$ and $\Delta(n,n',t)$, the quantities required for our test of the DTD picture at short t.

For the chain fully labeled at all monomeric segments, $I_s(\boldsymbol{q},t)$ is given by eq A1 with g being replaced by Ng and the summation $\sum_j$ being taken for all segments in the chain. The $1 - I_s$ vs q^2 plot made for this $I_s(\boldsymbol{q},t)$ gives the average mean-square displacement utilized in eq 27, $\overline{[\delta_{av}(t)]^2} = (1/gN)\sum_{j=1}^{gN}\langle[\Delta\boldsymbol{\rho}(j,t)]^2\rangle$.

References and Notes

(1) Marrucci, G. *J. Polym. Sci., Polym. Phys. Ed.* **1985**, *23*, 159.
(2) Ball, R. C.; McLeish, T. C. B. *Macromolecules* **1989**, *22*, 1911.
(3) Watanabe, H. *Prog. Polym. Sci.* **1999**, *24*, 1253.
(4) Milner, S. T.; McLeish, T. C. B. *Macromolecules* **1997**, *30*, 2159.

(5) Milner, S. T.; McLeish, T. C. B. *Macromolecules* **1998**, *31*, 7479.
(6) Milner, S. T.; McLeish, T. C. B. *Phys. Rev. Lett.* **1998**, *81*, 725.
(7) Doi, M.; Edwards, S. F. *The Theory of Polymer Dynamics*; Clarendon: Oxford, England, 1986.
(8) Matsumiya, Y.; Watanabe, H.; Osaki, K. *Macromolecules* **2000**, *33*, 499.
(9) Watanabe, H.; Matsumiya, Y.; Osaki, K. *J. Polym. Sci., Part B: Polym. Phys.* **2000**, *38*, 1024.
(10) Matsumiya, Y.; Watanabe, H. *Macromolecules* **2001**, *34*, 5702.
(11) Watanabe, H. *Korea-Aust. Rheol. J.* **2001**, *13*, 205.
(12) Watanabe, H.; Matsumiya, Y.; Inoue, T. *Macromolecules* **2002**, *35*, 2339.
(13) Inoue, T.; Okamoto, H.; Osaki, K. *Macromolecules* **1991**, *24*, 5670.
(14) Inoue, T.; Osaki, K. *Macromolecules* **1996**, *29*, 1595.
(15) Inoue, T.; Onogi, T.; Yao, M. L.; Osaki, K. *J. Polym. Sci., Part B Polym. Phys.* **1999**, *37*, 389.
(16) The prefactor of the integral in eq 20, $1/\pi^2\{(a' - a)/2\}^4$, was misprinted as $1/\pi^2(a'/2)^4$ in ref 12.
(17) Green, P. F.; Mills, P. J.; Palmstrϕm, C. J.; Mayer, J. W.; Kramer, E. J. *Phys. Rev. Lett.* **1984**, *53*, 2145.
(18) Kanaya, T.; Kaji, K. *Adv. Polym. Sci.* **2001**, *154*, 87.

MA021200T